

Excitation Spectrum and Correlation Functions of the \mathbb{Z}_3 -Chiral Potts Quantum Spin Chain

A. Honecker* and G. von Gehlen⁺

*Physikalisches Institut der Universität Bonn
Nussallee 12, 53115 Bonn, Germany*

Abstract : We study the excitation spectrum and the correlation functions of the \mathbb{Z}_3 -chiral Potts model in the *massive high-temperature phase* using perturbation expansions and numerical diagonalization. We are mainly interested in results for general chiral angles but we consider also the superintegrable case. For the parameter values considered, we find that the band structure of the low-lying part of the excitation spectrum has the form expected from a quasiparticle picture with *two* fundamental particles.

Studying the N -dependence of the spectrum, we confirm the stability of the second fundamental particle in a limited range of the momentum, even when its energy becomes so high that it lies very high up among the multiparticle scattering states. This is not a phenomenon restricted to the superintegrable line.

Calculating a non-translationally invariant correlation function, we give evidence that it is oscillating. Within our numerical accuracy we find a relation between the oscillation length and the dip position of the momentum dispersion of the lightest particle which seems to be quite independent of the chiral angles.

1 The \mathbb{Z}_3 -chiral Potts model

Recently, the \mathbb{Z}_n -symmetrical chiral Potts model [1, 2] has attracted particular interest [3]–[11]¹ because of its special integrability properties and the rich structure of its phase diagram. In this paper we consider the \mathbb{Z}_3 -quantum chain version of the model [12]. The Hamiltonian of the model contains complex coefficients and this gives rise to a large number of ground state- (and also higher level-) crossings, and to the appearance of both massive and massless oscillating phases. We present evidence that the spectrum has a quasiparticle structure all over the massive high-temperature phase. We also study the peculiar momentum dependent effects which appear due to the parity-noninvariance of the model: A quasiparticle may overlap with a two-particle spectrum for a limited range of its momenta. We investigate whether by immersing into the continuum the particle remains stable or ceases to exist as a quasiparticle. Such an effect has been discovered recently in [8] for the superintegrable case of the chiral Potts chain. Finally, we present finite-size calculations which establish directly an oscillatory behaviour of certain correlation functions in the massive high-temperature phase.

The \mathbb{Z}_3 -chiral Potts quantum chain with N sites is defined by the Hamiltonian:

$$H_N^{(3)} = -\frac{2}{\sqrt{3}} \sum_{j=1}^N \left\{ e^{-i\varphi/3} \sigma_j + e^{i\varphi/3} \sigma_j^\dagger + \lambda \left(e^{-i\phi/3} \Gamma_j \Gamma_{j+1}^\dagger + e^{i\phi/3} \Gamma_j^\dagger \Gamma_{j+1} \right) \right\}. \quad (1)$$

The operators σ_j and Γ_j act in a vector space \mathbb{C}^3 located at site j . They satisfy the relations

$$\sigma_i \Gamma_j = \Gamma_j \sigma_i \omega^{\delta_{j,j'}}; \quad \sigma_j^n = \Gamma_j^n = 1; \quad \text{where} \quad \omega = e^{2\pi i/3}. \quad (2)$$

We shall use the representation

$$\sigma_j = \begin{pmatrix} 1 & 0 & 0 \\ 0 & \omega & 0 \\ 0 & 0 & \omega^2 \end{pmatrix}_j, \quad \Gamma_j = \begin{pmatrix} 0 & 0 & 1 \\ 1 & 0 & 0 \\ 0 & 1 & 0 \end{pmatrix}_j. \quad (3)$$

In this paper we will consider the ferromagnetic case $0 \leq \lambda < \infty$. Using periodic boundary conditions $\Gamma_{N+1} = \Gamma_1$, the Hamiltonian (1) commutes with the translation operator T and with the \mathbb{Z}_3 -charge operator $\hat{Q} = \prod_{j=1}^N \sigma_j$. Their eigenvalues have the form e^{iP} and ω^Q , respectively, leading to conservation of the momentum P (which for finite chains takes the N discrete values $0 \leq 2\pi k/N < 2\pi$ with $k = 0, 1, \dots, N-1$), and to the conservation *mod* 3 of the charge $Q = 0, 1, 2$. See e.g. [1, 5] for the definition of the chiral Potts quantum chain for general \mathbb{Z}_n which for $n = 2$ reduces to the standard Ising quantum chain.

The \mathbb{Z}_3 -model contains three parameters: λ which plays the rôle of the inverse temperature, and ϕ, φ which are two chiral angles. For $\phi = \varphi = \frac{\pi}{2}$, the Hamiltonian (1) is ‘superintegrable’, i.e. it fulfills the Onsager algebra [1, 6]. For

$$\cos \varphi = \lambda \cos \phi \quad (4)$$

(1) has been shown to be integrable [3] due to a new type of Yang-Baxter equation which contains two rapidities *not* enjoying the usual difference property. For generic $\phi = \varphi$ the

¹For a more complete list of references see e.g. [7]

Hamiltonian (1) is self-dual but probably not integrable. The self-dual model is parity-invariant only for $\phi = \varphi = 0$. In this case (1) is just the standard \mathcal{WA}_2 -symmetrical \mathbb{Z}_3 -Potts quantum chain. The phase diagram of (1) contains four distinct phases, two of which are massless incommensurate phases. For recent reviews summarizing the known properties of the model, see [5, 9].

In this paper we shall study properties of the *massive high-temperature phase* of the model which occurs for small λ : $0 < \lambda < \lambda_c(\phi, \varphi)$. The boundary of this phase, $\lambda_c(\phi, \varphi)$, is known exactly only for a few special values of ϕ, φ : For $\phi = \varphi$, it is known that $\lambda_c(0, 0) = 1$ (standard Potts case), $\lambda_c(\frac{\pi}{2}, \frac{\pi}{2}) = 0.901292\dots$ (superintegrable case) [3] and for $\phi \rightarrow \pi, \varphi \rightarrow \pi$ we have $\lambda_c \rightarrow 0$ [12].

In Sec. 2 we start explaining our tools for analyzing the spectrum of (1), summarizing known formulae and presenting simple new perturbation formulae. In Sec. 3 we show that the finite-size data follow the band structure expected for a quasiparticle spectrum. In Sec. 4 we study the immersion of the $Q = 2$ -quasiparticle into the many-particle continuum for a limited range of P . In Sec. 5 we study a non-translationally invariant correlation function and establish its oscillatory nature which previously had been inferred only from wave-vector scaling arguments. A simple relation between the dip position of the $Q = 1$ -particle dispersion relation and the oscillation length is found to be approximately valid over a large parameter range. Finally, Sec. 6 presents our Conclusions.

2 Methods of calculation

The complete analytic calculation of the spectrum of (1) in the superintegrable case $\phi = \varphi = \frac{\pi}{2}$ by the Stony-Brook group ([8] and references therein) has established that for these parameter values the spectrum has a quasiparticle structure, i.e. in [8] it has been shown that in the large chain limit *all* excitations $\Delta E_{Q,r}(P, \lambda)$ above the ground state are composed of two fundamental excitations $E_1(P)$ and $E_2(P)$ according to the following rules:

$$\Delta E_{Q,r}(P, \lambda) = \sum_{k=1}^{m_r} E_{Q^{(k)}}(P^{(k)}), \quad P = \sum_{k=1}^{m_r} P^{(k)} \bmod 2\pi, \quad Q = \sum_{k=1}^{m_r} Q^{(k)} \bmod 3. \quad (5)$$

Additionally, the fundamental quasiparticles satisfy a Pauli principle, i.e.

$$Q^{(i)} = Q^{(j)} \quad \text{implies} \quad P^{(i)} \neq P^{(j)}. \quad (6)$$

For more general ϕ, φ and general \mathbb{Z}_n numerical results were presented in [10] which suggested that such a quasiparticle structure (with $n - 1$ quasiparticles in the \mathbb{Z}_n -case) is present all over the massive high-temperature phase. Here we want to give further evidence for such a structure for the \mathbb{Z}_3 model (1) for quite general ϕ, φ . For this we compare multi-particle levels to the basic single-particle levels and check whether the former can be composed out of the latter ones. Single-particle levels are expected to show exponential convergence in N to the thermodynamic limit, while composite states should show power convergence with the power indicating the number of constituents [9, 10].

In order to analyze the spectrum, three different approaches will be used:

1) In each charge-momentum sector we calculate numerically the lowest ≥ 10 energy levels of (1). For chains of length $N \leq 8$ complete numerical diagonalization is easily possible, while for up to $N \leq 12$ sites we use Lanczos techniques. This way, both the basic quasiparticle dispersion relations $E_1(P)$ and $E_2(P)$ and many continuum levels can be obtained. The limit $N \rightarrow \infty$ may be calculated using standard finite-size extrapolation techniques. In general, the convergence in N depends on the mass scale involved. For small λ the mass scale is large but also for λ close to $\lambda = 1$, where the mass scale is small, good information can be obtained as will be shown below.

2) Compact analytic, though approximate formulae for each *lowest* level in the $Q \neq 0$ sectors can be calculated for general ϕ and $-\frac{\pi}{2} < \varphi < \frac{\pi}{2}$ using perturbation theory in λ . We find up to order λ^3 :

$$\begin{aligned} E_1(P) &:= \Delta E_{1,0}(P, \phi, \varphi) \\ &= 4 \sin\left(\frac{\pi - \varphi}{3}\right) - \frac{4\lambda}{\sqrt{3}} \left\{ \mathcal{F}(P) + \alpha - 2\beta - (\alpha^2 + 2\beta^2) \cos \phi \right\} + \mathcal{O}(\lambda^4), \end{aligned} \quad (7)$$

with

$$\mathcal{F}(P) = (1 - A) \cos p + \alpha \cos(p + \phi) + \beta \cos(2p) + B \cos(2p + \phi) + 2\beta^2 \cos(3p), \quad (8)$$

where

$$p = P - \frac{\phi}{3}, \quad \alpha = \frac{\lambda}{6 \cos\left(\frac{\pi - \varphi}{3}\right)}, \quad \beta = \frac{\lambda}{6 \cos\left(\frac{\varphi}{3}\right)}, \quad (9)$$

and $A = 3\beta^2 - 2\alpha\beta + 2\alpha^2$; $B = 2\beta^2 + 2\alpha\beta - \alpha^2$. In the superintegrable case we have $\alpha = \beta = \lambda/(3\sqrt{3})$ and $A = B = \lambda^2/9$.

For $0 \leq \varphi < \frac{\pi}{2}$ the lowest $Q = 2$ excitation is given by:

$$E_2(P) := \Delta E_{2,0}(P, \phi, \varphi) = \Delta E_{1,0}(P, -\phi, -\varphi). \quad (10)$$

These formulae are expected to be valid for λ not too large, i.e. if the distance of the level from other multiparticle levels is not too small. Of course, this nondegenerate perturbation calculation is useless once a level penetrates into the continuum of multiparticle states. We shall see that there are parameter values for which this happens in the $Q = 2$ -sector.

The P -dependence of E_1 is contained in $\mathcal{F}(P)$ only. So, e.g. to find the value of the momentum $P = P_{\min}$, for which the lowest energy is reached (because of parity violation this is not at $P = 0$), we have to look for the solution of $\partial\mathcal{F}/\partial p = 0$. For non-zero ϕ , $\cos\frac{\pi - \varphi}{3}$ and $\cos\frac{\varphi}{3}$, we see that $p_{\min} \equiv P_{\min} - \frac{\phi}{3}$ is of order λ . So, expanding we get

$$P_{\min} = \frac{\phi}{3} - \alpha \sin \phi + \mathcal{O}(\lambda^2). \quad (11)$$

Observe that, in order to obtain P_{\min} to order λ , we have to use the second order expansion of $E_1(P)$. Starting for $\lambda \ll 1$ at $P_{\min} = \frac{\phi}{3}$, the position of the minimum shifts to smaller values of P for increasing λ . Using (10), one obtains immediately the minimum of the curve $E_2(P)$.

3) For the superintegrable case $\phi = \varphi = \frac{\pi}{2}$ analytic formulae are available from [8] for the whole spectrum. We shall use here only the formulae for the energies of the two

fundamental excitations which are given by

$$\begin{aligned} E_1(P_r) &= e_r = 2 |1 - \lambda| + \frac{3}{\pi} \int_1^{|\frac{1+\lambda}{1-\lambda}|^{2/3}} dt \frac{v_r(2v_r t + 1)}{v_r^2 t^2 + v_r t + 1} \sqrt{\frac{4\lambda}{t^3 - 1} - (1 - \lambda)^2} \\ E_2(P_{2s}) &= e_{2s} = 4 |1 - \lambda| + \frac{3}{\pi} \int_1^{|\frac{1+\lambda}{1-\lambda}|^{2/3}} dt \frac{v_{2s}(4v_{2s}^2 t^2 - v_{2s} t + 1)}{v_{2s}^3 t^3 + 1} \sqrt{\frac{4\lambda}{t^3 - 1} - (1 - \lambda)^2}, \end{aligned} \quad (12)$$

where the auxiliary variables v_r and v_{2s} are related to the momenta by:

$$v(P) = + \sqrt{\frac{1 - \cos P}{1 - \cos(P + \frac{2\pi}{3})}}, \quad (13)$$

$$v_{2s}(P) = -v(2\pi - P), \quad v_r(P) = \begin{cases} -v(P) & \text{for } 0 \leq P \leq 4\pi/3; \\ +v(P) & \text{for } 4\pi/3 \leq P \leq 2\pi. \end{cases} \quad (14)$$

The integral appearing in $E_2(P_{2s})$ has a singularity at $P = 2\pi/3$, so that the $Q = 2$ -quasiparticle level is defined only for $2\pi/3 \leq P \leq 2\pi$. Except for this singularity, there is no problem to evaluate the integrals in (12) numerically: using $\xi = \sqrt{t - 1}$ instead of t as our integration variable, the integrands are smooth at $\xi = 0$ or $t = 1$.

Comparing these different methods, we can keep control about the precision of the values to be used for $E_1(P)$ and $E_2(P)$ for all ϕ, φ and $\lambda < 1$. We shall comment on such comparisons as we go on presenting our results. Methods 1) and 2) can be applied equally well also in the non-integrable and in the non-hermitian situation (the Lanczos method can also be adapted to the case of non-hermitian matrices [14]) which arises for complex ϕ or φ e.g. if (4) is imposed. This way we can cover a large range of ϕ and φ .

As a first example, from which one can judge the usefulness of the different methods, in Fig. 1 we show the lowest part of the $Q = 1$ -spectrum for the superintegrable case $\phi = \varphi = \frac{\pi}{2}$ at the large value of $\lambda = 0.90$ which is close to the phase transition point. We see that the finite-size data for $N = 12$ lie still within $< 6\%$ on the exact curve (12). For small P , even the points for small N move nicely along the exact curve. Of course, with only $N \leq 12$ we cannot get directly points in the interval $0 < P < \pi/6$. Considering the large value of λ and the vicinity of the phase transition, it is remarkable that the 3rd-order perturbation curve remains close to the exact curve, especially for $P > 1.2\pi$. It mainly fails to describe details of the dip at small P , and so is not useful for the determination of the transition to the incommensurate (IC)-phase (where the ground state loses translational invariance).

3 Quasiparticle- and band-structure of the spectrum

In order to investigate the band structure expected from the composition of the two quasiparticles, in Fig. 2 we start considering the simple situation which occurs for a small value of λ , here in particular $\lambda = 0.1$, and a self-dual choice of the chiral angles $\phi = \varphi = \frac{\pi}{4}$ well below the superintegrable line. The single-particle dispersion curves can be determined with high precision: the $N = 12$ finite-size value for $E_1(P)$ agrees to better than 10^{-4} with the value given by formula (7). Also the agreement in $E_2(P)$ between $N = 12$ and perturbation theory is better than 10^{-3} over the whole range

of P . Both curves are rather flat, corresponding to a large mass in a Klein-Gordon-type approximation to the dispersion curve. Of course, at $\lambda = 0$ the P -dependence is completely absent, as is immediately seen from the perturbation expansion.

From these single-particle dispersion curves we can calculate the shape of the two-particle bands in all three charge Q -sectors. These bands are bounded by $E_Q^\pm(P)$, given by

$$E_Q^+(P) = \max_{-\pi < q \leq \pi} \{E_{Q_1}(P/2 + q) + E_{Q_2}(P/2 - q)\}, \quad Q = Q_1 + Q_2 \bmod 3 \quad (15)$$

(and similarly $E_Q^-(P)$ with \max_q replaced by \min_q). Now, as long as the P -dependence of the quasiparticle dispersion curves has the form

$$E_{Q_i}(P) = A_i + \sum_j B_{ij} \cos(P - \alpha_{ij}), \quad (16)$$

the boundaries $E_Q^\pm(P)$ for two *equal* particles are obtained for $q = 0, \pi$, respectively, and we have simply

$$E_Q^\pm(P) = E_{Q_1}(P/2) + E_{Q_2}(P/2). \quad (17)$$

Of course, we have to use the doubled Brillouin zone for P . In the perturbation formula (7) the first term to spoil the form (16) is the term $\sim \lambda^2 \cos(2P - \frac{2\phi}{3})$. For the parameters chosen in Fig. 2 this is quite small. For two charge conjugate particles (in our \mathbb{Z}_3 -case this occurs for $Q = 0$), with $\alpha_{1,j} = -\alpha_{2j}$ and $A_1 = A_2$, $B_{1j} = B_{2j}$ (which is true in order λ of (7), (10)), we get

$$E_1(P/2 + q) + E_2(P/2 - q) = 2 \left\{ A_1 + \sum_j B_{1,j} \cos(P/2) \cos(q - \alpha_{ij}) \right\}. \quad (18)$$

so that the band width becomes zero at $P = \pi$. The λ^2 -contributions no longer obey fully (16) with the effect that the lower corner of the zero-width point is rounded off.

In Fig. 2 we have plotted the nine lowest $N = 12$ -sites levels of each charge and each momentum state. As expected in the quasiparticle picture, we see that at all available values of $P \neq \pi$ there are three bunches of levels with the correct charge filling up and following the respective two-particles band ranges. The P -values, where the respective bands have zero width is nicely seen to be at $P = \pi \pm 2P_{\min} \approx \pi \pm \pi/6$ for the $Q = 2$ - and $Q = 1$ -bands, respectively, and at $P = \pi$ for the $Q = 0$ -band. For $Q = 1$ and $Q = 2$, according to whether k is odd or even, the uppermost three, respective two highest levels start forming the next bands which at these energies are expected from three-particles states.

Only for $P = \pi$ four $Q = 0$ -points appear outside of the bands. The two points slightly above $E = 8$ are within the expected three-particle band but the two points above and below $E = 6.5$ must be two-particle states which, because of power convergence at $N = 12$, are still out of the here very narrow band. Such finite-size effects have been discussed in detail for $P = 0$ in [10]. There we found that, taking finite-size effects into account, for $P = 0$ the quasiparticle picture explains the data very well.

In Fig. 3 we show the analogous picture for a somewhat larger value of the inverse temperature, $\lambda = 0.25$, and a (again self-dual) choice of the chiral angles $\phi = \varphi = 67.5^\circ$, closer to the superintegrable value $\phi = \varphi = 90^\circ$. For the $Q = 1$ -ground state the

third order perturbation formula still agrees within $\approx 10^{-3}$ over the whole range of the momentum with the $N = 12$ sites data, however, there are somewhat larger ($\approx 5 \cdot 10^{-2}$) discrepancies for the lowest $Q = 2$ -level.

The band structure in all three charge sectors is of the same shape as before and all higher levels lie within the bands (this time we show *all* higher levels for $N = 4, \dots, 12$ sites but draw only the boundary curves for the $Q = 2$ - band). The approximation (17) for the *lower* bound of the $Q = 2$ -two particle band is no longer perfect, it is interesting to see that the finite-size data at the most narrow point $P \approx 1.22\pi$ do follow the curvature expected. With increasing N the bands are filled densely from the *interior* which is consistent with but of course no proof of the presence of the Pauli principle effect (6).

More important is to observe in this Figure that, due to the parity non-invariance, the maximum of the E_2 -curve is shifted to the left of $P = \pi$, while the two- $Q = 1$ -particle band is shifted to the right of $P = \pi$. This causes the curve for E_2 to penetrate into the two-particle band. This may make the $Q = 2$ -quasiparticle unstable in a limited range of the momentum around $P \approx 2\pi/3$. Indeed, the convergence with N of the lowest level in the $Q = 2$ -sector deteriorates considerably at these momenta.

In [9, 10] it has been pointed out that the $Q = 2$ -particle enters the continuum composed out of two $Q = 1$ -particles at $P = 0$ on the superintegrable line. However, we see that for $P \approx 2\pi/3$ this effect appears already for lower values of ϕ . With increasing λ this "threshold" moves to smaller values of ϕ . It is tempting to suspect that the limitation of the range of the momentum for the $Q = 2$ -quasiparticle discovered in [8] for the superintegrable case, see eq. (12), might be due to this penetration effect. In the following Section we try to shed some light on this problem by studying the chain-size-dependence of the spectrum.

Not surprising in view of the penetration of the $Q = 2$ -quasiparticle into the continuum, the perturbation formula for $E_2(P)$ of eqs. (7), (10), which for $\lambda = 0.25$ and $\phi = \varphi = 67.5^\circ$ was still good, becomes quite useless for larger values of λ and ϕ : E.g. for $\lambda = 0.5$ and $\phi = \varphi = 60^\circ$ it is off by 20 – 25% around $P = 0$, while in the backward direction it describes the finite-size data still within $< 3\%$. Going at $\lambda = 0.5$ to $\phi = \varphi = 75^\circ$, in the forward direction the λ^3 -perturbation formula value is already too large by about a factor of three (only around $1.2\pi \leq P \leq 1.5\pi$ the curve comes back to the finite-size data within a few percent).

Looking again into Fig. 1 we see that there are ten points which appear well below the curve $E_1(P)$. This happens because close to $\lambda = 1$ also the $Q = 1$ -quasiparticle enters a multiparticle band. This time the band is formed by four of the same $Q = 1$ -particles as can be seen by estimating its lower boundary from $E_1(P - 3P_{\min}) + 3E_1(P_{\min})$. So it is not trivial that the perturbation formula for $E_1(P)$ remains useful around $\lambda \approx 0.9$ as seen in Fig. 1.

4 Stability of the $Q = 2$ -quasiparticle in the two-particle continuum

4.1 The superintegrable case

As we have seen, the description of the $Q = 2$ -quasiparticle by perturbation theory breaks down as the chiral angles approach the superintegrable value $\phi = \varphi = \frac{\pi}{2}$. This,

of course, is related to the overlapping of the $Q = 2$ -particle with the continuum. At $\phi = \varphi = \frac{\pi}{2}$, where for $P = 0$ the $Q = 2$ -particle sits just at the threshold of the two $Q = 1$ -particle scattering states (sometimes expressed in the form that for these chiral angles $m_2 = 2m_1$ [9]). Since one can guess the correct diagonal linear combination of states at this point for $0 \leq \lambda < 1$, degenerate perturbation theory is possible here [13]. However, it is not known how to generalize this at $\phi = \varphi = \frac{\pi}{2}$ to $P \neq 0$, because in the standard basis the diagonal combination of states probably is highly complicated.

Finite-size methods are not affected by these problems and still give good information (these will be useful even for $\varphi > \frac{\pi}{2}$, $\phi > \frac{\pi}{2}$) as we shall see by comparison to the exact $N \rightarrow \infty$ formula (12). In particular, we are going to check now whether we can confirm the details of the peculiar energy-momentum rule of the $Q = 2$ -quasiparticle (12) by finite-size calculations. After showing that this is possible, we go ahead and look whether a similar unusual energy-momentum rule is also found for non-superintegrable chiral angles. The question whether integrability plays a special rôle here will be studied choosing chiral angles for which the system probably is not integrable.

Fig. 4 shows the curves calculated from (12) together with the 9 lowest $N = 12$ finite-size eigenvalues for each Q, P for $\phi = \varphi = \frac{\pi}{2}$ and $\lambda = 0.50$ which is right in the center of the high-temperature phase.

In the lower part of Fig. 4 we see the curve $e_r(P)$ drawn according to the analytic formula (12). The $Q = 1, N = 12$ -data (crosses) lie within $< 2 \cdot 10^{-5}$ on this curve ².

The small dashed lines mark the two-particle band expected for two $Q = 1$ -quasiparticles according to both (15) (rounded lower curve at $P \approx 1.3\pi$) and the approximation (17) (crossing curves). For $P < 3\pi/2$ the $Q = 2$ -particle dips into the two-particle band, which for finite- N (consider only the $Q = 2$ -squares in the Figure) contains many states. Studying their N -dependence one finds that in general these points move considerably when N is varied, indicating an only power-convergence to the thermodynamic limit. However, one notices that e_{2s} neatly *passes through* several $N = 12$ -finite-size eigenvalues which for $P \leq 4\pi/3$ are some of the higher lying levels. We are now going to argue that it is no random coincidence that the e_{2s} -curve passes through the $N = 12$ -points but this comes because these states belong to an exponentially converging sequence, characteristic of a fundamental quasiparticle (For the concept of a quasiparticle see the beginning of Sec. 2).

Exponential convergence for states of fixed momentum P can be inferred from finite-size data directly only if a sequence of different N -values at the same P is accessible. Since $P = 2\pi k/N$, with k integer, this is possible e.g. for $P = \pi$, where we can use data for all even N .

However, being limited to $N \leq 12$, there are only a few other values of P where more than one N can be used, e.g. $P = 2\pi/3$ which is reached for $N = 12, 9, 6, 3$ with $k = 4, 3, 2, 1$. Table 1 gives such data for the case $\lambda = 0.5$ of of Fig. 4. We compare the convergence in N of the high-lying $Q = 2$ -levels which are very close to the curve e_{2s} with the lowest $Q = 1$ -data. About the $Q = 1$ -levels we are on quite safe grounds to assume that these approximate the well-isolated $Q = 1$ -quasiparticle exponentially fast for $N \rightarrow \infty$. Table 1 shows clearly that the convergence in N to the high-lying $Q = 2$ -levels is practically as good as that of the $Q = 1$ -levels and consequently also

²Also the $E_1(P)$ -third order perturbation curve (7) (not shown in the Figure) agrees still within $< 2\%$ with the exact expression. Observe that the λ here is much smaller than the $\lambda = 0.9$ chosen in Fig. 1. Compare also the fourth columns in Tables 1 and 2 below.

P	$Q = 1$			$Q = 2$		
	e_r	Finite chain	Perturb.	e_{2s}	Finite chain / level #	
$\frac{\pi}{6}$	0.8659401	0.8659349 $N = 12$	0.855991			
$\frac{\pi}{3}$	1.1875666	1.1875601 $N = 12$	1.157407			
$\frac{\pi}{2}$	1.7400548	1.7400475 $N = 12$	1.741481			
$\frac{2\pi}{3}$	2.3110674	2.3110599 $N = 12$	2.333333	6.0000000	5.9999978 $N = 12/8th$	
		2.3108898 $N = 9$			5.9998044 $N = 9/5th$	
		2.3099686 $N = 6$			5.9963767 $N = 6/4th$	
$\frac{5\pi}{6}$	2.7776630	2.7776545 $N = 12$	2.784303	5.7768864	5.7725860 $N = 12/7th$	
π	3.0691561	3.0691471 $N = 12$	3.064815	5.4748476	5.4754941 $N = 12/7th$	
		3.0690841 $N = 10$			5.4727480 $N = 10/5th$	
		3.0687830 $N = 8$			5.4797166 $N = 8/5th$	
$\frac{7\pi}{6}$	3.1472946	3.1472849 $N = 12$	3.144009	5.0141793	5.0139793 $N = 12/6th$	
$\frac{4\pi}{3}$	3.0000000	2.9999893 $N = 12$	2.990741	4.3971362	4.3972296 $N = 12/5th$	
		2.9998304 $N = 9$			4.3960055 $N = 9/4th$	
		3.0002000 $N = 6$			4.3984911 $N = 6/3rd$	
$\frac{3\pi}{2}$	2.6408227	2.6408101 $N = 12$	2.628890	3.6717090	3.6216780 $N = 12/1st$	
		2.6405539 $N = 8$			3.6716026 $N = 8/2nd$	
$\frac{5\pi}{3}$	2.1133290	2.1133098 $N = 12$	2.111111	2.9355387	2.9353258 $N = 12/1st$	
		2.1176771 $N = 6$			2.9386269 $N = 6/1st$	
$\frac{11\pi}{6}$	1.5070578	1.5070792 $N = 12$	1.511994	2.3525974	2.3572572 $N = 12/1st$	
2π	1.0000000	0.9999978 $N = 12$	1.009260	2.0000000	1.9999893 $N = 12/1st$	
		0.9999851 $N = 11$			1.9999701 $N = 11/1st$	
		0.9999405 $N = 10$			1.9999247 $N = 10/1st$	

Table 1: Comparison of the exact formulae (12) with finite chain size data for $N = 12$ and less sites and with the $3rd$ -order perturbation formula for $\lambda = 0.50$ and $\phi = \varphi = \frac{\pi}{2}$ (superintegrable case). In the last column we indicate how high up in its $(Q = 2, P)$ -sector the quoted energy level appears. For $Q = 1$ the finite- N -values are always the $Q = 1$ -ground state ($1st$) levels.

exponential. This way we can trace the $Q = 2$ -quasiparticle, if it is present, over its whole range of the momentum by our finite-size methods. Although at other values of P (e.g. $P = 7\pi/6$) we have only one "measurement" for $N = 12$, we conclude from the closeness of the $N = 12$ -value to the exact result that also here we probably have exponential convergence. In contrast, in the case of power convergence, typically the $N = 12$ -values are off the $N \rightarrow \infty$ -limit still by several percent.

We like to emphasize that the choice of levels, even if we get very high up in the spectrum, in practically all cases is quite unambiguous: e.g. for $\lambda = 0.5$ and $P = \frac{2\pi}{3}$ the next neighbouring levels to those quoted in Table 1 are: for $N = 12$: 5.8192/6.0000/6.1965, for $N = 9$: 5.6962/5.9998/6.2942 and for $N = 6$: 5.3865/5.9964/7.8306. For $\lambda = 0.5$ and $P = \pi$ at $N = 12$ we have the neighbours 5.2154/5.4755/5.9303 which are also well separated. That we are not victims of coincidences will be very clear from Fig. 5 below and also from Table 2 which gives the analogous results for $\lambda = 0.90$. Here, since we are much closer to the phase transition line, the level structure is much more involved. Nevertheless, although the mass scale of the system is smaller by a factor 5 as compared to $\lambda = 0.5$ (as a relevant scale we may consider $E_1(P = 0) = 2(1 - \lambda)$), and we have to go up to the 26th level at $P = 2\pi/3$ and $N = 12$, the convergence is still excellent.

Notice that the convergence is not monotonous in N but with oscillations superimposed, a phenomenon quite common in the chiral Potts model [9].

To show that *below* $P = 2\pi/3$ there is *no* exponentially converging level is not so easy because we do not know precisely where to search. We cannot search in the immediate neighbourhood below $P = 2\pi/3$, because for $N \leq 13$ sites (with some effort, $N = 13$ -chains can be calculated but are quite useless here since 13 is a prime number), the next lowest point where we can test for fast convergence is $P = \pi/2$. There we do not see any convincingly close levels in the $N = 12$, $k = 3$ and $N = 8$, $k = 2$ -spectra. A better argument that $P = 2\pi/3$ is the lower endpoint of the $Q = 2$ -quasiparticle with respect to P will be given below in connection with Fig. 4, using the change of the spectrum at $P = 2\pi/3$ with ϕ , φ when moving away from the superintegrable line.

Summarizing, we see that even from our numerical studies one obtains strong evidence that one can interpret the spectrum of (1) on the superintegrable line in terms of two elementary quasiparticles with energies $e_r(P)$ and $e_{2s}(P)$. The unusual features of the $Q = 2$ quasiparticle are clearly reflected in the finite-size data. Decreasing P from 2π towards lower values, the $Q = 2$ excitation crosses the scattering threshold of two $Q = 1$ excitations at some point but stays stable.

4.2 The non-superintegrable case

We expect that the limitation of the $Q = 2$ -quasiparticle to only part of the range of the momentum should not only appear at the superintegrable line $\phi = \varphi = \frac{\pi}{2}$ but by continuity should be valid, maybe with changing range, also for neighbouring values of ϕ and φ .

From our earlier calculations in [10] we get a hint about the endpoint at $P = 2\pi$: For $\phi = \varphi > \frac{\pi}{2}$ this endpoint should move to $P < 2\pi$ because we found that the $Q = 2$ -particle becomes unstable at $P = 0$ (or $P = 2\pi$) (which was the only value for P considered there).

In order to get more information, we now study the $Q = 2$ spectra at $P = 2\pi/3$ for $N = 6, 9, 12$ sites as functions of the chiral angle ϕ at fixed $\lambda = 0.50$. In order to vary

P	$Q = 1$			$Q = 2$		
	e_r	Finite chain	Perturb.	e_{2s}	Finite chain / level #	
$\frac{\pi}{6}$	0.224478	0.226286 $N = 12$	-0.0161071			
$\frac{\pi}{3}$	1.064266	1.069278 $N = 12$	0.8840000			
$\frac{\pi}{2}$	2.016074	2.022656 $N = 12$	2.1927771			
$\frac{2\pi}{3}$	2.882061	2.889695 $N = 12$	3.0800000	7.600000	7.5955496 $N = 12/26th$	
		2.915791 $N = 9$			7.595578 $N = 9/11th$	
		3.003151 $N = 6$			7.608462 $N = 6/5th$	
$\frac{5\pi}{6}$	3.551636	3.560115 $N = 12$	3.5107612	7.251272	7.237896 $N = 12/21th$	
		3.961730 $N = 12$			6.797425	6.7850878 $N = 12/17th$
π	3.952458	3.977025 $N = 10$	3.8360000	6.797425	6.778859 $N = 10/10th$	
		4.010626 $N = 8$			6.795053 $N = 8/7th$	
		4.040930 $N = 12$			6.114959	6.100765 $N = 12/14th$
$\frac{7\pi}{6}$	3.800000	3.811210 $N = 12$	3.8000000	5.190112	5.176061 $N = 12/6th$	
		3.843411 $N = 9$			5.173303 $N = 9/4th$	
		3.950279 $N = 6$			5.218181 $N = 6/3rd$	
$\frac{3\pi}{2}$	3.238310	3.251180 $N = 12$	3.2112229	4.056564	4.041591 $N = 12/3rd$	
		3.310811 $N = 8$			4.050302 $N = 8/3rd$	
$\frac{5\pi}{3}$	2.389589	2.405991 $N = 12$	2.3600000	2.777609	2.763267 $N = 12/2nd$	
		2.592734 $N = 6$			2.804678 $N = 6/1st$	
$\frac{11\pi}{6}$	1.316212	1.352448 $N = 12$	1.2452388	1.450685	1.438850 $N = 12/1st$	
		0.200000			0.187664 $N = 12$	0.400000
2π	0.200000	0.186542 $N = 11$	0.2000000	0.400000	0.418118 $N = 11/1st$	
		0.186060 $N = 10$			0.428335 $N = 10/1st$	

Table 2: Comparison of the exact formulae (12) with finite chain size data for $N \leq 12$ sites and with the $3rd$ -order perturbation formula for $\lambda = 0.90$ and $\phi = \varphi = \frac{\pi}{2}$ (super-integrable case). In the last column we indicate how high up in its ($Q = 2, P$)-sector the particular quoted energy level appears. In contrast to Table 1, here for $Q = 1$ the levels approximating the curve $E_1(P)$ are not always the $Q = 1$ -ground state levels. Recall Fig. 1 which showed that the $Q = 1$ -quasiparticle is entering the continuum for $2\pi/3 \leq P \leq \pi$.

only one parameter, we have used both the self-dual choice $\phi = \varphi$ and the integrable choice (4) but we found that both behave very similarly. So here we present only results for the self-dual case. For this choice (1) probably is not integrable, and the effects we are going to see should not be due to the integrability.

In Fig. 5 one clearly distinguishes three curves, one for each $N = 6, 9, 12$, which follow each other very closely for $\phi \geq 90^\circ$ and separate in the region $\phi < 90^\circ$. At $\phi = 90^\circ$ this is the $Q = 2$ -particle of (12), and the three values for $N = 6, 9, 12$ are those of Table 1 (5.9999978 *etc.*). Notice that indeed there are no other levels close to 6.000 around $\phi = 90^\circ$, and that nowhere else in the picture are lines from $N = 6, 9, 12$ following closely the same course. We see that the $Q = 2$ -quasiparticle curve can be followed uniquely up to $\phi = 125^\circ$, and that the fast convergence from $N = 6$ to $N = 12$ is still there. Around $\phi \approx 120^\circ$ the convergence is quite perfect. The energy values at $\phi = 120^\circ$ being 5.57251; 5.57211; 5.57192 for $N = 6, 9, 12$, respectively.

For larger angles the $Q = 2$ -quasiparticle level gets so high up in the spectrum that computational problems limit to follow it for $N = 12$: at $\phi = 126^\circ$ it is already the 30th level in its sector. In Fig. 5 we have plotted up to the 29th $N = 12$ -level in the $Q = 2, P = 2\pi/3$ -sector. Around $\phi \approx 100^\circ$ the convergence is somewhat worse but still quite good: 5.81200; 5.79749; 5.79150 at $\phi = 99^\circ$. We interpret this as continuing presence and stability of the $Q = 2$ -quasiparticle for $90^\circ \leq \phi < 125^\circ$ at $P = 2\pi/3$.

However, for $\phi < 90^\circ$ the curves for $N = 6, 9, 12$ clearly separate. We consider this to be an indication that here the $Q = 2$ -particle gets out of its stability range. This is consistent with the analytic result that for $\phi = \varphi = \frac{\pi}{2}$, $P = 2\pi/3$ is the lower momentum bound of the second quasiparticle.

On the scale on which Fig. 5 is drawn it is difficult to show that apparent crossings of level-lines with the same N, Q and P are in fact avoided crossings, since the levels come very close to each other. E.g. consider the $N = 9$ -levels which around $\phi \approx 99.035^\circ$ seem to cross at $E \approx 5.797$. At their closest encounter they keep separated in energy by $\Delta E \approx 0.0007911$.

It remains to see what happens above the superintegrable line for other momenta. E.g. for $P = \pi$ we find that the three $Q = 2$ -levels for $N = 8, 10, 12$, which were very close to each other for $\phi = \varphi = \frac{\pi}{2}$, stay very close together if we move in ϕ . Table 3 gives a few numbers for the energy of the $Q = 2$ -particle obtained by following this triple. At intermediate momentum values, where we have only one $N \leq 12$ available, we can make use of a property which is clearly seen in Fig. 5 but which is qualitatively the same for other P , too: the levels approximating the $Q = 2$ -quasiparticle have a slope $\partial E_2/\partial \phi$ which is very different from that of other levels. Using this feature we can follow the quasiparticle line to larger ϕ , starting from the known value at $\phi = \varphi = \frac{\pi}{2}$. Of course, when using just this method we have no direct control over the size of errors.

In order to illustrate that the integrable case is analogous to the self-dual one for the parameters under consideration we also mention two further values of $E_2(P)$: For the *integrable* choice of parameters $\lambda = 0.50$, $\varphi = 114^\circ$ one finds $E_2(P = 2\pi/3) = 5.683(2)$ and $E_2(P = \pi) = 5.30608(3)$. Note the similarity between these two values including their errors with the corresponding ones in Table 3.

We conclude this Section with the remark that for small λ the behaviours of the self-dual ($\phi = \varphi$) and the integrable versions (4) *have* to be different, because in the integrable case for small λ the non-hermitian region comes close to the line $\phi = \varphi = \frac{\pi}{2}$, whereas in the self-dual case little special is happening for small λ when moving in ϕ

$\phi = \varphi$	90°	96°	102°	108°	114°	120°
$P = 2\pi/3$	6.0000(1)	5.84(1)	5.745(5)	5.687(7)	5.626(2)	5.5718(3)
$P = \pi$	5.475(1)	5.4261(5)	5.3827(2)	5.34024(6)	5.29667(4)	5.25038(5)

Table 3: $Q = 2$ -quasiparticle energies at $\lambda = 0.50$ for two values of the momentum P and varying chiral angles $\phi = \varphi$. The values in the Table are estimates for the limit $N \rightarrow \infty$ obtained from the values at $N = 12, 9, 6$ and $N = 12, 10, 8$ sites, respectively.

around $\phi = \frac{\pi}{2}$.

5 Correlation functions

In this Section we define and study a non-translationally invariant correlation function for the operator Γ of the \mathbb{Z}_3 -chain numerically. We shall use the definition

$$C_\Gamma(x) := \frac{\langle v | \Gamma_{x+1}^+ \Gamma_1 | v \rangle}{\langle v | v \rangle} \quad 0 \leq x < \frac{N}{2} \quad (19)$$

where $|v\rangle$ is the lowest eigenvector of the Hamiltonian in the sector $Q = P = 0$ which in the massive high-temperature phase is the ground state. The definition (19) ensures $C_\Gamma(-x) = C_\Gamma(x)^*$. Non-translationally invariant correlation functions are difficult to measure experimentally but for our purpose it will be crucial to work really with $\Gamma_{x+1}^+ \Gamma_1$ and *not* to replace it by $N^{-1} \sum_{r=1}^N \Gamma_{x+r}^+ \Gamma_r$, because this would destroy the oscillation.

Because we are studying a massive phase, we expect an exponential decay in addition to the oscillatory contribution. So a simple ansatz for $C_\Gamma(x)$ may be made in terms of a complex correlation length or equivalently, in terms of the real correlation length ξ_Γ and the oscillation length L defined through

$$C_\Gamma(x) = ae^{2\pi ix/L} e^{-x/\xi_\Gamma} + (1-a)\delta_{x,0}. \quad (20)$$

For the massive *low-temperature* phase a non-vanishing wave vector has been predicted in [9] where also its critical exponent was calculated from level crossings. Perturbative calculations of the correlation function $C_\Gamma(x)$ for the massive low-temperature phase have been performed in [11] and indications for an oscillatory contribution have been obtained. Detailed perturbative studies of $C_\Gamma(x)$ in the massive *high-temperature* phase will be presented in [13].

We have noticed in [10] that in the high-temperature limit, the dispersion curve of the $Q = 1$ -particle has its minimum at $P_{\min} = \text{Re}\phi/3$, as it is obvious from the term of first order in λ of $E_1(P)$, see eq. (7). The value of P_{\min} decreases with increasing λ : e.g. for $\phi = \varphi = \pi/2$ one finds from (12), (14) that at $\lambda = 0.901292$ $P_{\min} \approx 0.225$ ³ so that at this λ , P_{\min} has diminished by a factor of ≈ 2.33 from its value at small λ . In Sec. 2 (see Fig. 1) we have also noticed that for large λ the third order formula (7) does not describe the dispersion curve around the minimum.

³More precise parameter values for the transition to the IC phase for $\phi = \varphi = \frac{\pi}{2}$ are: $\lambda = 0.90129284\dots$, $P_{\min} = 0.22503375(3)$.

The non-zero shift of the minimum of the dispersion curve has the result that at $\phi \neq 0$, already for $\lambda \rightarrow 0$, the first excited state is no longer at $P = 0$. For a finite N -site chain with chain momentum $k = NP/2\pi$, the lowest gap has $\Delta k = [NP_{\min}/2\pi]$. This gives rise to a proliferation of cross-overs in the first excited states with increasing N which in turn, via finite-size scaling arguments [15], indicates an oscillating $\Delta P \neq 0$ correlation function. So we may expect P_{\min} to be related to the oscillation length L of the correlation function.

For $\lambda \rightarrow 0$ this relation is readily found using a high-temperature expansion for the correlation function (19). Calculating (19) up to second order in λ , we obtain

$$C_{\Gamma}(x) = \delta_{x,0} + \lambda \delta_{x,1} \frac{e^{i\phi/3}}{3 \cos(\frac{\varphi}{3})} + \frac{\lambda^2}{12 \cos^2(\frac{\varphi}{3})} \left\{ \delta_{x,1} e^{-2i\phi/3} + 2\delta_{x,2} e^{2i\phi/3} \right\} + \mathcal{O}(\lambda^3). \quad (21)$$

In order to extract the complex correlation length from this formula to lowest nontrivial order, we consider

$$\frac{C_{\Gamma}(2)}{C_{\Gamma}(1)} = \frac{e^{i\phi/3}}{2 \cos(\frac{\varphi}{3})}. \quad (22)$$

On the other hand, from (20) we have

$$\frac{C_{\Gamma}(2)}{C_{\Gamma}(1)} = \exp\left(\frac{2\pi i}{L} - \frac{1}{\xi_{\Gamma}}\right), \quad (23)$$

so that, comparing (22) with (23) we obtain

$$L \operatorname{Re}\phi = 6\pi, \quad \xi_{\Gamma}^{-1} = \frac{\operatorname{Im}\phi}{3} - \ln \frac{\lambda}{2 \cos(\frac{\varphi}{3})}. \quad (24)$$

(We write $\operatorname{Re}\phi$, since e.g. in the integrable case (4) ϕ can be complex for small λ). Using the small- λ expression for P_{\min} , the first of these equations can be rewritten as a relation between the oscillation length L and the minimum P_{\min} of the dispersion relation (7):

$$P_{\min}L = 2\pi, \quad (25)$$

which is valid at general ϕ , φ and small inverse temperatures λ .

In the following, we will show that with a finite-size numerical calculation, using up to 13 sites, one can get useful information on the oscillation length L at various values of the parameters in the high-temperature phase. Since, as we have seen, L is conceptually linked to P_{\min} , we shall conveniently give our results in terms of the product $P_{\min}L$. It will turn out that (25) seems to be satisfied approximately for a wide range of parameters.

In order to evaluate the correlation function (19) numerically, one needs the ground state of the Hamiltonian (1). The ground state of the \mathbb{Z}_3 -chain is easily obtained for general values of the parameters (even in the non-hermitian case $\phi \in \mathbb{C}$ [14]) using vector iteration up to $N = 13$ sites. The more difficult point is to calculate the matrix elements of $\Gamma_{x+1}^+ \Gamma_1$, because this operator does not conserve momentum and thus does not leave a space of momentum eigenstates invariant. Table 4 shows the correlation function $C_{\Gamma}(x)$ obtained in this manner for $N = 12$ and $N = 13$ sites at two different points in the phase diagram: first for $\lambda = 0.5$ in the superintegrable case, and second, for $\lambda = 0.25$ and the chiral angle φ above the superintegrable line and ϕ chosen complex (so that the Hamiltonian becomes non-hermitian) satisfying the integrability condition (4).

	$\phi = \varphi = \frac{\pi}{2}, \lambda = 0.50$		$\varphi = \frac{3\pi}{4}, \phi = \pi + 1.70005i, \lambda = 0.25$	
x	<i>12 sites</i>	<i>13 sites</i>	<i>12 sites</i>	<i>13 sites</i>
0	1	1	1	1
1	.18881 + .07385 <i>i</i>	.18882 + .07385 <i>i</i>	.06242 + .10811 <i>i</i>	.06242 + .10811 <i>i</i>
2	.04587 + .03967 <i>i</i>	.04588 + .03967 <i>i</i>	-.01305 + .02260 <i>i</i>	-.01305 + .02260 <i>i</i>
3	.01004 + .01737 <i>i</i>	.01007 + .01738 <i>i</i>	-.00668	-.00667 + .00000 <i>i</i>
4	.00126 + .00679 <i>i</i>	.00132 + .00684 <i>i</i>	-.00096 - 0.00167 <i>i</i>	-.00096 - .00165 <i>i</i>
5	-.00056 + .00224 <i>i</i>	-.00043 + .00242 <i>i</i>	.00032 - .00056 <i>i</i>	.00028 - .00052 <i>i</i>
6	-.00080	-.00063 + .00058 <i>i</i>	.00037	.00022 - .00005 <i>i</i>

Table 4: Numerical results for the correlation function $C_\Gamma(x)$ at $N = 12, 13$ sites

The excellent agreement between the calculations at $N = 12$ and $N = 13$ sites shows that the contribution of boundary terms to the correlation functions is small. So we can use the $N = 12$ -values as a good approximation for the infinite chain limit as long as $x \leq 6$.

We thus obtain six complex numerical values for C_Γ at each fixed point (λ, ϕ, φ) in the phase diagram considered. By a fitting procedure, we want to translate these six values into the three parameters ξ_Γ , L and a of (20). We proceed as follows: First, we obtain ξ_Γ by calculating $\text{Re}(\ln(C_\Gamma(x)/C_\Gamma(x+1)))^{-1}$ and averaging over x . Next, the first zero of $\text{Re}(e^{x/\xi_\Gamma} C_\Gamma(x))$ is estimated by linear interpolation for two neighbouring values and $L/4$ is obtained by averaging. Finally, a is chosen such that the difference

$$\text{Re}C_\Gamma(x) - ae^{-x/\xi_\Gamma} \cos(2\pi x/L) \quad (26)$$

is minimal for $x = 1, 2$. Table 5 collects our results for 12 choices of λ and the chiral angles.

For the entries marked with a ‘*’ $\text{Re}C_\Gamma$ does not yet reach zero in the interval $[0,6]$. Here we calculated L from the formula

$$L = \frac{1}{4} \sum_{x=1}^4 \frac{2\pi}{\text{Im}(\ln(C_\Gamma(x)/C_\Gamma(x+1)))}. \quad (27)$$

The values of P_{\min} in Table 5 have been obtained by first calculating $E_1(P)$ numerically at $N = 12$ sites and afterwards minimizing the finite Fourier decomposition of $(E_1(P))^2$ numerically - compare also Table 8 of [10]. These values are approximations with errors which are difficult to estimate.

The eighth and ninth line in Table 5 give situations close to, and *in* the IC phase. In both cases $E_1(P)$ partly enters two-particle scattering states. For $\phi = \varphi = \frac{3\pi}{4}$, $\lambda = \frac{3}{4}$ we are in the IC-phase with $E_1(P)$ becoming negative. We nevertheless define the correlation function for these cases with $|v\rangle$ still denoting the $Q = P = 0$ -ground state, although it is no longer the lowest state of (1). Since in these cases the method explained above for estimating P_{\min} becomes impractical, here we proceeded differently: We first determine

φ	ϕ	λ	ξ_Γ	L	a	P_{\min}	$LP_{\min}/2\pi$
$\frac{3\pi}{8}$	$\frac{3\pi}{8}$	$\frac{1}{4}$	0.53(3)	18(2)	0.65(3)	0.341	1.0(1)
$\frac{3\pi}{8}$	$\frac{3\pi}{8}$	$\frac{1}{2}$	0.8(2)	25(1)*		0.283	1.14(6)
$\frac{3\pi}{8}$	$\frac{3\pi}{8}$	$\frac{3}{4}$	1.8(6)	$50 \pm 23^*$		0.211	1.7(8)
$\frac{\pi}{2}$	$\frac{\pi}{2}$	$\frac{1}{4}$	0.6(1)	14.05(6)	0.44(8)	0.470	1.051(4)
$\frac{\pi}{2}$	$\frac{\pi}{2}$	$\frac{1}{2}$	0.60(5)	16(1)	0.59(3)	0.401	1.07(8)
$\frac{\pi}{2}$	$\frac{\pi}{2}$	$\frac{3}{4}$	1.3(2)	29(6)*		0.189	0.9(2)
$\frac{3\pi}{4}$	$\frac{3\pi}{4}$	$\frac{1}{4}$	0.62(8)	10(1)	0.4(2)	0.746	1.18 ± 0.12
$\frac{3\pi}{4}$	$\frac{3\pi}{4}$	$\frac{1}{2}$	1.2(6)	12(1)	0.4(1)	0.685 [†]	1.34 ± 0.14
$\frac{3\pi}{4}$	$\frac{3\pi}{4}$	$\frac{3}{4}$	1.4(1)	16(1)	0.65(3)	0.602 [†]	1.54(8)
$\frac{3\pi}{8}$	$-0.98942i$	$\frac{1}{4}$	0.7(2)	∞		0	
$\frac{3\pi}{8}$	0.69919	$\frac{1}{2}$	1.1(3)	49(7)*		0.159	1.2(2)
$\frac{3\pi}{4}$	$\pi + 1.70004i$	$\frac{1}{4}$	1.0(5)	5.9(1)	0.3(1)	$\frac{\pi}{3}$	0.99(2)

Table 5: Parameters for the correlation function (20) calculated numerically for $N = 12$ sites. In the first nine lines we give data for the choice $\phi = \varphi$ of the chiral angles, where three lines correspond to the superintegrable case $\phi = \varphi = \frac{\pi}{2}$. The bottom three lines use the integrable choice (4).

the smallest energy gap in the $Q = 1$ sector at $N = 8, \dots, 12$ which appears at the smallest value possible for the discrete momentum, $P = 2\pi/N$. Next, a polynomial interpolation between these five values for the energy gap was minimized numerically. In Table 5 we marked these results by ‘†’.

At the end of Table 5 we give three examples with integrable choices of the chiral angles (4). For $\varphi = \frac{3\pi}{8}$, $\lambda = \frac{1}{2}$, the integrable Hamiltonian is still hermitian and behaves very similarly to the self-dual case. However, for small values of λ and $\phi \neq \pi/2$, one has to make one of the angles φ , ϕ complex in order to satisfy (4). We choose ϕ complex. Below the superintegrable line $\phi = \varphi = \frac{\pi}{2}$ one can take ϕ purely imaginary, whereas above the superintegrable line one has to admit a non-vanishing real part, e.g. $\phi - \pi \in i\mathbf{R}$. With these choices one can verify, using e.g. (7), that $\mathbf{E}_1(-P) = \mathbf{E}_1(P)^*$ for $\varphi < \frac{\pi}{2}$ and imaginary ϕ (for details, see [14]). Therefore, it seems sensible to set $P_{\min} = 0$, and, if (25) holds at least approximately, we expect no oscillation. Indeed, the complete correlation function $C_\Gamma(x)$ is real for the integrable choice of parameters $\varphi = \frac{3\pi}{8}$, $\lambda = \frac{1}{4}$ which in view of (20), implies $L = \infty$. For the integrable point $\varphi = \frac{3\pi}{4}$, $\lambda = \frac{1}{4}$ above the superintegrable line we have verified that (7) and a numerical evaluation of $\mathbf{E}_1(P)$ at $N = 12$ sites satisfy $\mathbf{E}_1(-P - \frac{\pi}{3}) = \mathbf{E}_1(P - \frac{\pi}{3})^*$. Thus, we set $P_{\min} = \frac{\pi}{3}$ which gives excellent agreement with the prediction $LP_{\min} = 2\pi$.

That the above procedures yield reasonable fits is demonstrated by Fig. 6 which shows the stretched correlation function $e^{x/\xi_\Gamma} C_\Gamma(x)$ obtained numerically for $N = 13$ sites at the integrable point $\varphi = \frac{3\pi}{4}$, $\lambda = \frac{1}{4}$ in comparison to the fits. The errors have been estimated from the difference between the results for $N = 12$ and $N = 13$ sites in Table 4. The agreement for all x , not only in the real part but also in the imaginary

part is good. In particular, the oscillation is clearly visible.

The conjecture $LP_{\min} = 2\pi$ is well verified for all values in Table 5, bearing in mind that we have ignored systematic errors. This may apply also to the point $\phi = \varphi = \frac{3\pi}{4}$, $\lambda = \frac{3}{4}$ in the massless IC phase, if we had underestimated the error in the determination of L .

6 Conclusions

In this paper we have presented further numerical evidence that the spectrum of the general \mathbb{Z}_3 -spin quantum chain (1) in the massive high-temperature phase can be interpreted in terms of two fundamental quasiparticles and their scattering states. Using duality [11] our results about the quasiparticle spectra can be pulled over to the massive low-temperature phase.

The quasiparticle carrying \mathbb{Z}_3 -charge $Q = 2$ shows a quite peculiar energy-momentum relation. It becomes unstable for a certain range of the momentum, while exhibiting a remarkable stability against decay into multi-particle states allowed by energy-momentum conservation in other ranges of the momentum. Since we find this feature not only in the superintegrable case, this generalizes the analytic result found by the Stony-Brook group [8] to cases for which no exact methods are known.

We also calculated the correlation function for the operator Γ using a numerical evaluation of the ground state of the \mathbb{Z}_3 -model for up to 13 sites. Although this approach is limited to short ranges, we are able to estimate correlation lengths in the massive high-temperature phase and can show that the correlation functions oscillate. We find that the product of the oscillation length L and the minimum of the dispersion curve P_{\min} (which is non-zero due to parity violation) satisfies $LP_{\min} \approx 2\pi$.

Acknowledgement We like to thank Fabian Eßler and Karim Yildirim for useful discussions.

References

- [1] G. von Gehlen, V. Rittenberg, \mathbb{Z}_n -Symmetric Quantum Chains with an Infinite Set of Conserved Charges and \mathbb{Z}_n Zero Modes, Nucl. Phys. **B257** (1985) p. 351
- [2] H. Au-Yang, B.M. McCoy, J.H.H. Perk, S. Tang, M.-L. Yan, Commuting Transfer Matrices in the Chiral Potts Models: Solutions of the Star-Triangle Equations with Genus > 1 , Phys. Lett. **A123** (1987) p. 219
- [3] G. Albertini, B.M. McCoy, J.H.H. Perk, Eigenvalue Spectrum of the Superintegrable Chiral Potts Model, Adv. Studies in Pure Math. **19** (1989) p. 1
- [4] G. Albertini, B.M. McCoy, J.H.H. Perk, Level Crossing Transitions and the Massless Phases of the Superintegrable Chiral Potts Chain, Phys. Lett. **A139** (1989) p. 204
- [5] B.M. McCoy, *The Chiral Potts Model: From Physics to Mathematics and Back*, Proceedings Special Functions - ICM 90, Satellite Conf., ed. M. Kashiwara and T. Miwa (Springer 1991) p. 245
- [6] B. Davies, *Onsager's Algebra and Superintegrability*, Jour. Phys. A: Math. Gen. **23** (1990) p. 2245
- [7] R. Kedem and B.M. McCoy, *Quasi-particles in the Chiral Potts Model*, preprint ITPSB 94-013, *hep-th/9405089*
- [8] S. Dasmahapatra, R. Kedem, B.M. McCoy, *Spectrum and Completeness of the 3 State Superintegrable Chiral Potts Model*, Nucl. Phys. **B396** (1993) p. 506
- [9] G. von Gehlen, *Phase Diagram and Two-Particle Structure of the \mathbb{Z}_3 -Chiral Potts Model*, Proceedings of *International Symposium on Advanced Topics of Quantum Physics*, ed. J.Q. Liang, M.L. Wang, S.N. Qiao, D.C. Su, Science Press Beijing (1992) p. 248
- [10] G. von Gehlen, A. Honecker, *Multi-Particle Structure in the \mathbb{Z}_n -Chiral Potts Models*, Jour. Phys. A: Math. Gen. **26** (1993) p. 1275
- [11] N.S. Han, A. Honecker, *Low-Temperature Expansions and Correlation Functions of the \mathbb{Z}_3 -Chiral Potts Model*, Jour. Phys. A: Math. Gen. **27** (1994) p. 9
- [12] S. Howes, L.P. Kadanoff, M. denNijs, *Quantum Model for Commensurate-Incommensurate Transitions*, Nucl. Phys. **B215** (1983) p. 169
- [13] A. Honecker, *A Perturbative Approach to the Chiral Potts Model*, preprint BONN-TH-94-21, *hep-th/9409122*
- [14] K. Yildirim, work in progress
- [15] C. Hoeger, G. von Gehlen, V. Rittenberg, *Finite-Size Scaling for Quantum Chains with an Oscillatory Energy Gap*, Jour. Phys. A: Math. Gen. **18** (1985) p. 1813

Figure captions

Fig. 1: Momentum dependence of the spectrum of the superintegrable \mathbb{Z}_3 -Hamiltonian in the $Q = 1$ -sector for $\lambda = 0.90$. Symbols: Finite chain data, dashed curve: exact lowest level from [3], point-dashed curve: $3rd$ -order perturbation in λ according to eq. (7).

Fig. 2: Spectrum of the \mathbb{Z}_3 -Hamiltonian at $\phi = \varphi = \frac{\pi}{4}$, $\lambda = 0.10$. All three charge sectors have been plotted in the same figure. The dots indicate eigenvalues for $N = 12$ sites whereas the lines are obtained from the $3rd$ -order perturbative expansions (7) and (10). We have limited ourselves to show for each (Q, P) the nine lowest eigenvalues only. One observes that the eigenvalues nicely group within the band boundaries expected according to (15). For $Q = 1$ and $Q = 2$ the first levels building up the three-particle bands are seen for $E > 8.5$. For a discussion of the four $Q = 0$ -points at $P = \pi$ outside the $(E_1 + E_2)$ -band, see the text.

Fig. 3: Same as Fig. 2 but for $\phi = \varphi = \frac{3\pi}{8}$, $\lambda = 0.25$. Note that all three charge sectors have been plotted in the same figure. Thus, seemingly overlapping bands belong to different charge sectors and so are no real level crossings. The dots indicate eigenvalues for $N = 4, \dots, 12$ sites. The curves show the perturbative results for $E_1(P)$ (full curve), $E_{Q=2}^\pm(P)$ (see eq. (15), long dashes) and $E_2(P)$ (fine dashes), according to (7), (10).

For some range of P the $Q = 2$ excitation enters the energy band of two $Q = 1$ particles. In this region, the $Q = 2$ "particle" is difficult to trace, although outside this region the convergence in N is very fast. This indicates that the $Q = 2$ fundamental excitation is not stable for all momenta P .

Fig. 4: Spectrum of the superintegrable \mathbb{Z}_3 -Hamiltonian at $\phi = \varphi = \frac{\pi}{2}$, $\lambda = 0.5$. All three charge sectors have been plotted in the same figure but only $N = 12$ -finite-size data are shown. The dashed curves show the analytic result of [8], eq. (12) for $2E_1(P/2)$ (long dashes) and $E_{Q=2}^\pm(P)$ (fine dashes). The full curve is the analytic result for $E_2(P)$. Note that the $Q = 2$ fundamental particle exists only for $P \geq \frac{2\pi}{3}$.

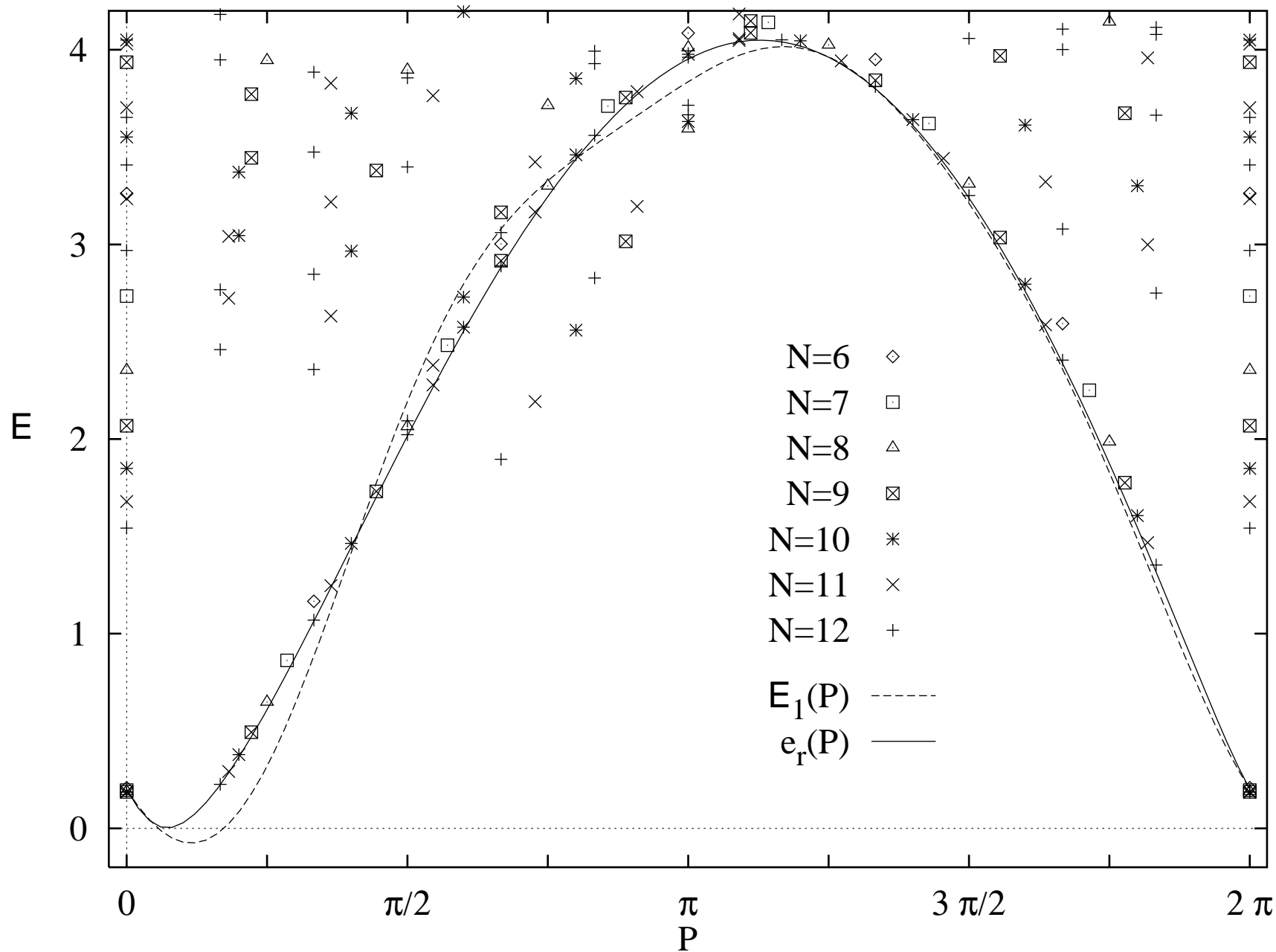
Fig. 5: Part of the spectrum in the $Q = 2$ -sector at $\lambda = 0.50$ and fixed momentum $P = 2\pi/3$ for $N = 6, 9, 12$ sites, as a function of the chiral angle $\phi = \varphi$ (self-dual choice). One sees that just one level from $N = 6, 9, 12$ each moves very closely together with their companions from the other N when ϕ varies. We take this as evidence for an exponential convergence of this level in N , characteristic for a single-particle state. In the upper right corner there are more $N = 12$ -levels which have not been drawn since we limited ourselves to calculate for $N = 12$ no more than 29 levels.

Fig. 6: Numerical values for the correlation function $C_\Gamma(x)$ at $N = 13$ sites stretched by e^{x/ξ_Γ} in comparison to the fit (20) at $\phi = \frac{3\pi}{4}$, $\lambda = \frac{1}{4}$, $\phi = \pi + 1.70004i$. The error bars are given by the differences between $N = 12$ and $N = 13$ sites. The parameters used for the fit are $\xi_\Gamma = 0.77$, $L = 6$ and $a = 0.35$. One observes that the agreement with these fits is good and the oscillatory contribution to $C_\Gamma(x)$ is clearly visible.

This figure "fig1-1.png" is available in "png" format from:

<http://arxiv.org/ps/hep-th/9409170v1>

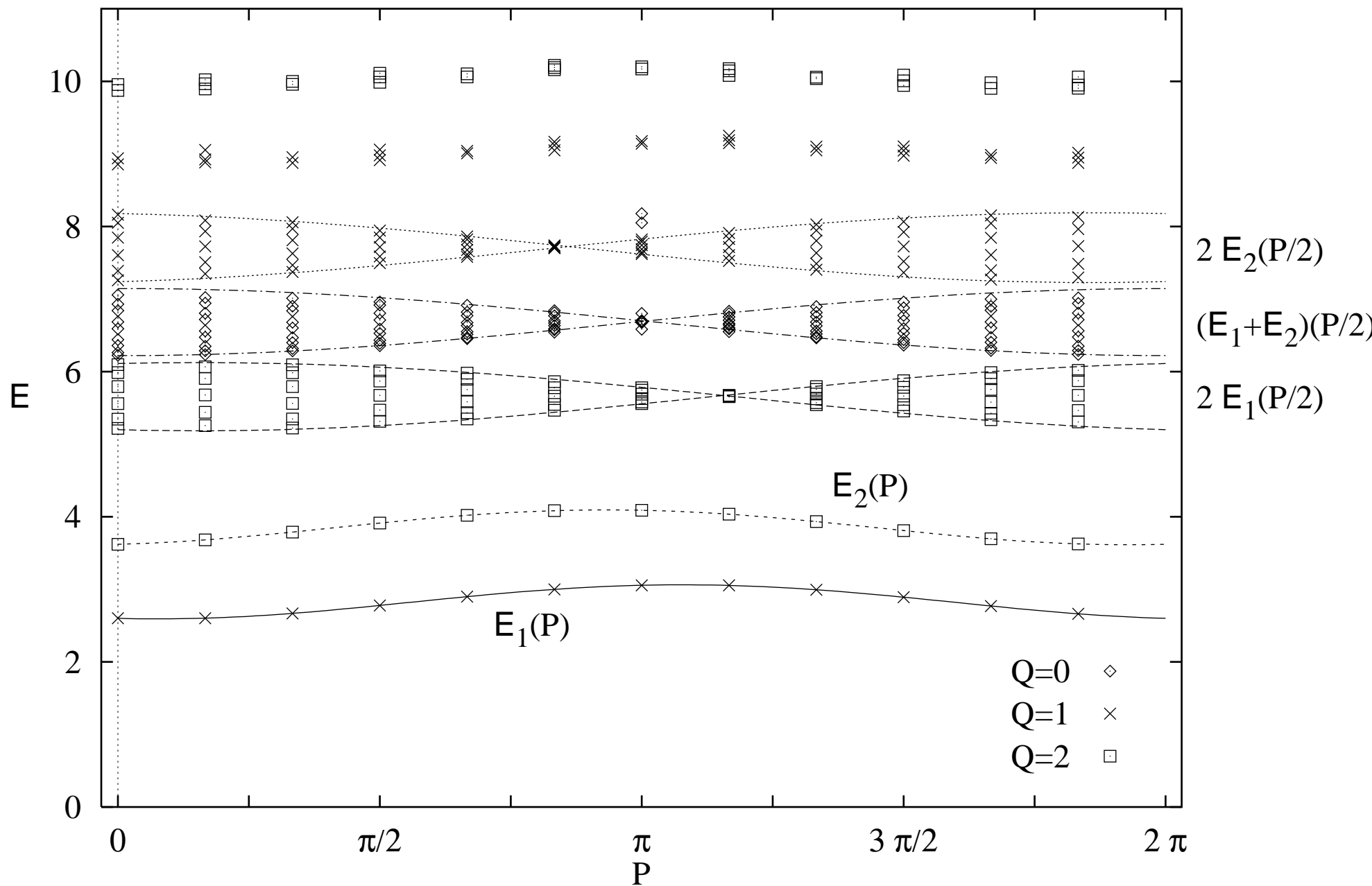
Fig. 1: Spectrum of the $Q=1$ sector at $\phi = \varphi = \pi/2, \lambda = 9/10$



This figure "fig1-2.png" is available in "png" format from:

<http://arxiv.org/ps/hep-th/9409170v1>

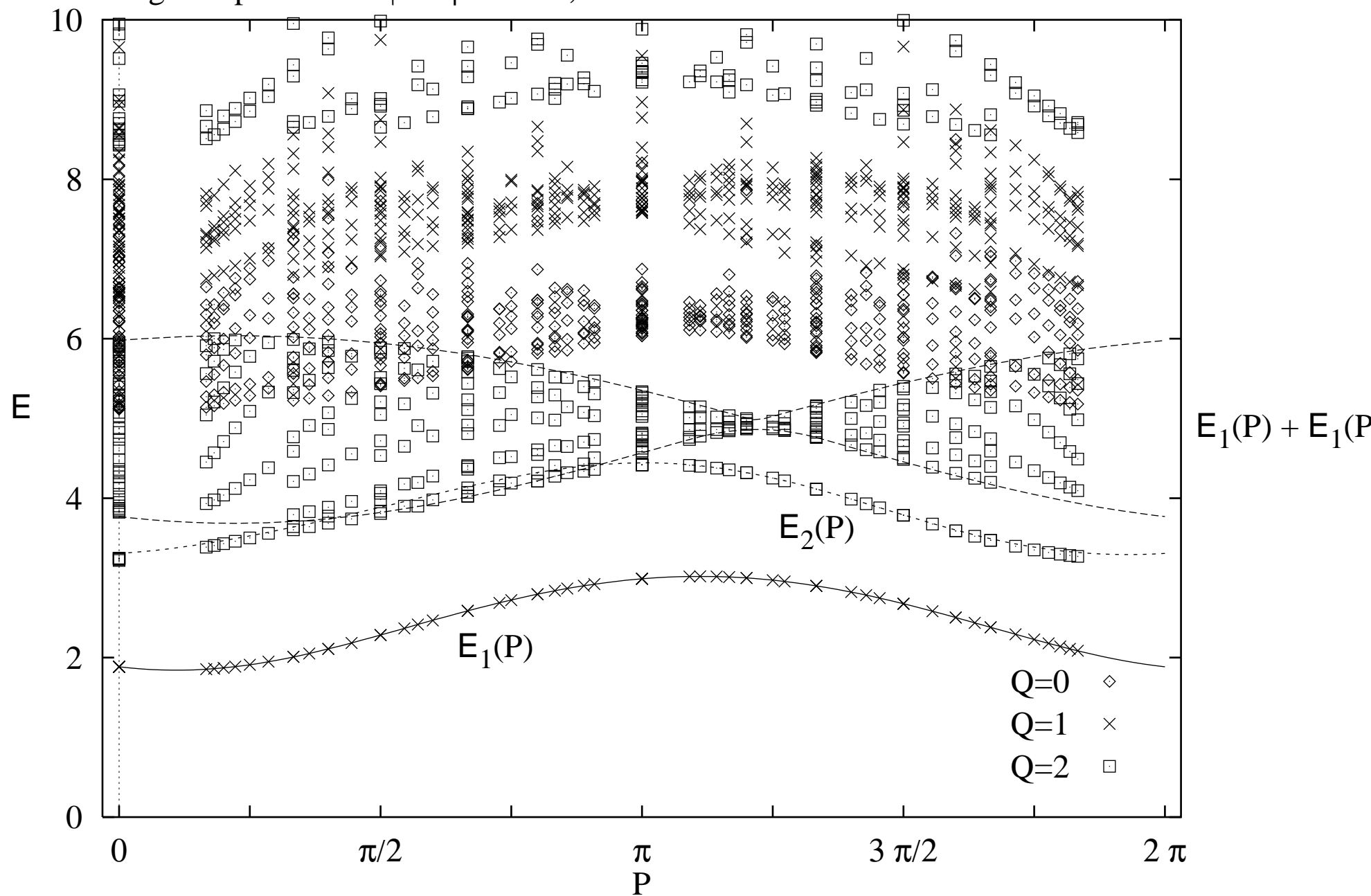
Fig. 2: Spectrum at $\phi = \varphi = \pi/4$, $\lambda = 1/10$



This figure "fig1-3.png" is available in "png" format from:

<http://arxiv.org/ps/hep-th/9409170v1>

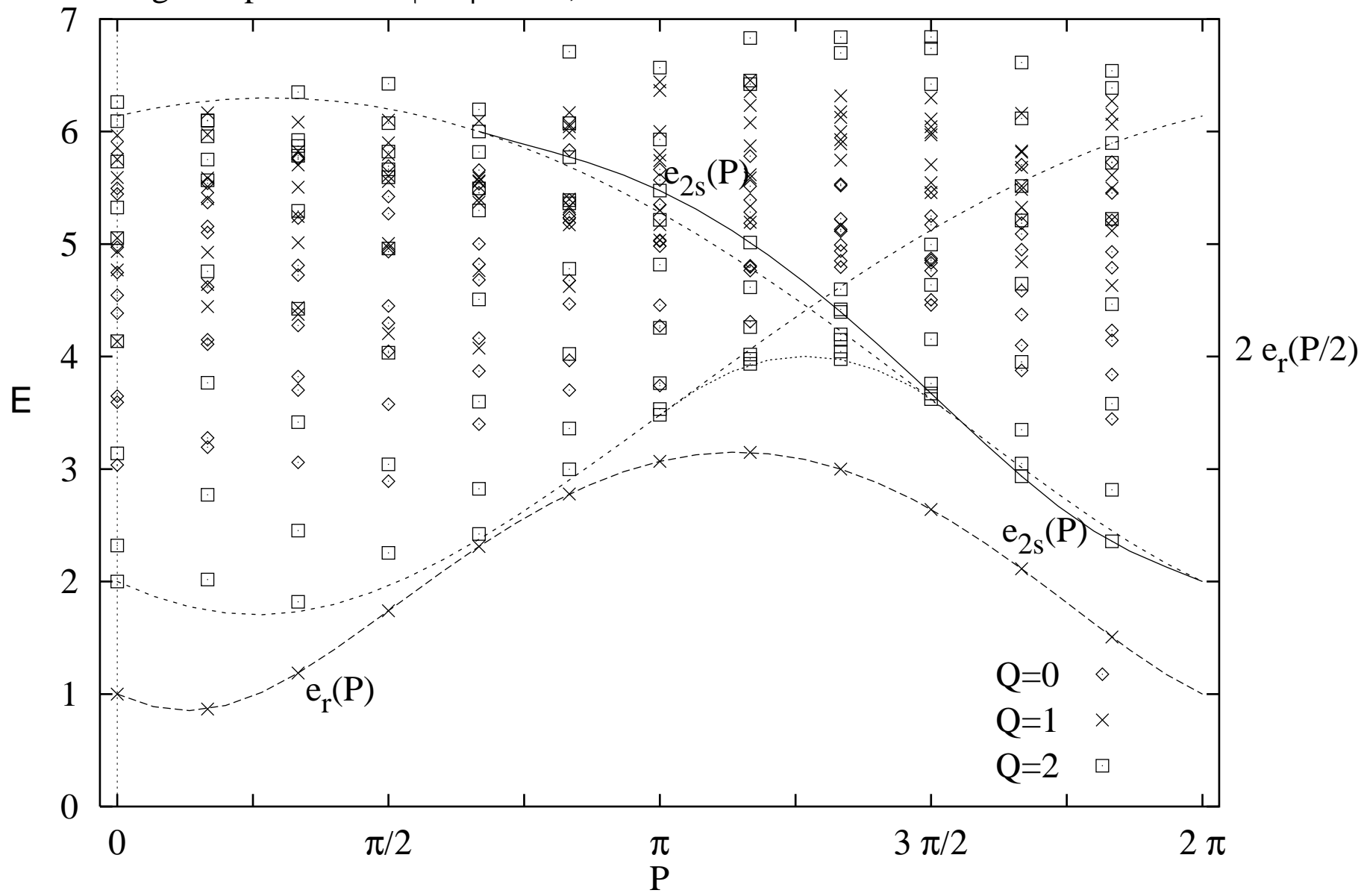
Fig. 3: Spectrum at $\phi = \varphi = 3 \pi/8, \lambda = 1/4$



This figure "fig1-4.png" is available in "png" format from:

<http://arxiv.org/ps/hep-th/9409170v1>

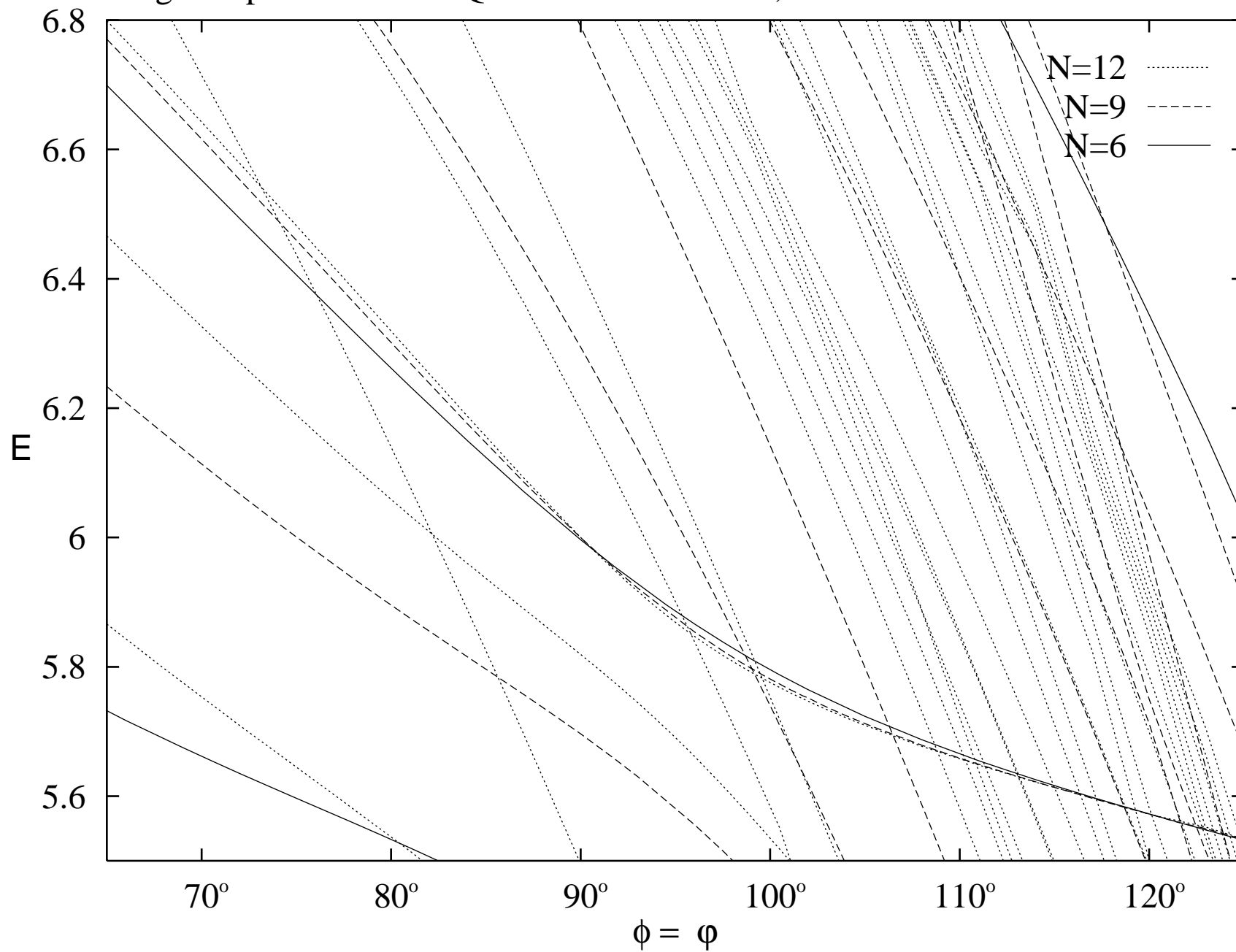
Fig. 4: Spectrum at $\phi = \varphi = \pi/2$, $\lambda = 1/2$



This figure "fig1-5.png" is available in "png" format from:

<http://arxiv.org/ps/hep-th/9409170v1>

Fig. 5: Spectrum of the $Q=2$ sector for $\lambda = 1/2$, $P=2 \pi/3$



This figure "fig1-6.png" is available in "png" format from:

<http://arxiv.org/ps/hep-th/9409170v1>

Fig. 6: Correlation for Γ at the integrable point $\varphi = 3\pi/4$, $\lambda = 1/4$, $\phi = \pi + i 1.70004$

